Article

TRANSPARENT PROCESS

EMBO reports

RNF123 has an E3 ligase-independent function in RIG-I-like receptor-mediated antiviral signaling

Shuai Wang, Yong-Kang Yang, Tao Chen, Heng Zhang, Wei-Wei Yang, Sheng-Sheng Song, Zhong-He Zhai & Dan-Ying Chen*

Abstract

Retinoic acid-inducible gene I (RIG-I) and melanoma differentiation-associated gene 5 (MDA5) are cytoplasmic sensors crucial for recognizing different species of viral RNAs, which triggers the production of type I interferons (IFNs) and inflammatory cytokines. Here, we identify RING finger protein 123 (RNF123) as a negative regulator of RIG-I and MDA5. Overexpression of RNF123 inhibits IFN-β production triggered by Sendai virus (SeV) and encephalomyocarditis picornavirus (EMCV). Knockdown or knockout of endogenous RNF123 potentiates IFN-β production triggered by SeV and EMCV, but not by the sensor of DNA viruses cGAS. RNF123 associates with RIG-I and MDA5 in both endogenous and exogenous cases in a viral infection-inducible manner. The SPRY and coiled-coil, but not the RING, domains of RNF123 are required for the inhibitory function. RNF123 interacts with the N-terminal CARD domains of RIG-I/MDA5 and competes with the downstream adaptor VISA/MAVS/IPS-1/Cardif for RIG-I/MDA5 CARD binding. These findings suggest that RNF123 functions as a novel inhibitor of innate antiviral signaling mediated by RIG-I and MDA5, a function that does not depend on its E3 ligase activity.

Keywords IFN-β; innate immunity; MDA5; RIG-I; RNF123
Subject Categories Immunology; Microbiology, Virology & Host Pathogen Interaction; Post-translational Modifications, Proteolysis & Proteomics
DOI 10.15252/embr.201541703 | Received 4 November 2015 | Revised 9 May 2016 | Accepted 19 May 2016 | Published online 16 June 2016
EMBO Reports (2016) 17: 1155–1168

Introduction

The innate immune reactions against pathogens invasion are mediated by host pattern-recognition receptors, which include Toll-like receptors (TLRs), RIG-I-like receptors (RLRs), nucleotide-binding oligomerization domain-like receptors (NLRs), and C-type lectin receptors [1]. The RLR family consisting of retinoic acid-inducible gene I (RIG-I), melanoma differentiation-associated gene 5 (MDA5), and laboratory of genetics and physiology 2 (LGP2) functions as the cytosolic viral RNA sensor, giving rise to downstream signals. Activated transcription factors interferon regulatory factor 3 (IRF3) and nuclear factor-kappaB (NF-κB) collaborate to trigger the transcription of type I interferons (IFNs) and pro-inflammatory cytokines, which contribute to the host antiviral immune responses [2–6]. RIG-I and MDA5 identify different RNA viruses. RIG-I recognizes Sendai virus (SeV), Newcastle disease virus (NDV), and vesicular stomatitis virus, whereas MDA5 responds to encephalomyocarditis picornavirus (EMCV) [3,4]. However, LGP2 is reported to play different regulatory roles in RIG-I or MDA5 signaling [7,8].

RIG-I and MDA5 contain an intensively conserved domain structure including two caspase activation and recruitment domains (CARDs) at the N-terminus, which mediate signaling to downstream adaptors, a DExD-box RNA helicase domain and a C-terminal domain (CTD), which is also known as the repressor domains [8,9]. Once the CTD recognizes viral RNA, RIG-I/MDA5 changes conformation to expose the CARDs, which combine with mitochondrial adaptor VISA/MAVS/IPS-I/Cardif [10–15]. This interaction triggers the aggregation of VISA (virus-induced signaling adaptor) [16] and then activates the TBK1 and TAK1 kinases. TBK1 (TANK-binding kinase 1) phosphorylates the transcription factor IRF3, causing IRF3 dimerization and translocation to promote the transcription of IFNs. However, TAK1 (TGFβ-activated kinase 1) phosphorylates IκB kinase (IKK) which activates the transcription factor NF-κB to induce the transcription of inflammatory cytokines [17,18].

Recently, cyclic GMP-AMP synthase (cGAS) has been determined as a cytosolic viral DNA sensor [19–21]. cGAS could recognize the viral DNA and synthesize cGAMP using cellular GTP and ATP [22,23]. Binding with cGAMP, the adaptor STING (stimulator of interferon genes) recruits TBK1 and IRF3, which activates the transcription of IFNs [24,25].

To prevent the excessive outcomes of immune responses, the activation procedure of RIG-I and MDA5 should be strictly controlled. Previous studies have suggested that RIG-I controls its basal activity by autoinhibition. Upon viral infection, the double-stranded viral RNA which contains 5′ triphosphate can be recognized by RIG-I and induce a conformational change of RIG-I to expose the CARDs to downstream adaptor proteins [10,11]. Protein modifications and the competitive combination are also indispensable for regulating the activity of RIG-I and MDA5. The E3 ubiquitin ligases TRIM25 and REUL/Riplet independently catalyze the Lys63 (K63) polyubiquitination and activation of RIG-I [26–29], whereas RNF125 mediates the Lys48 (K48) polyubiquitination and

Key Laboratory of Cell Proliferation and Differentiation of The Ministry of Education, School of Life Sciences, Peking University, Beijing, China
*Corresponding author. Tel: +86 1062757924; E-mail: dychen@pku.edu.cn

degradation of RIG-I and MDA5 by proteasome [30]; CYLD, which has been deemed as deubiquitinating enzyme, could negatively regulate RIG-I-mediated signaling, whereas another deubiquitinating enzyme USP17 plays a positive role in regulating RLR signaling [31,32]. The regulators of the autophagy, Atg5–Atg12 conjugate, inhibit RIG-I signaling via direct interaction with the CARD domain of RIG-I and VISA [33].

In the present study, we performed a yeast two-hybrid screen and received a RING finger protein, RNF123, as a novel RIG-I/MDA5 interactor. RNF123 is also known as KPC1, which is demonstrated to be a component of the Kip1 ubiquitination-promoting complex (KPC) heterodimer. The other component is KPC2 (UBAC1). The KPC promotes the degradation of P27Kip1 which is the cyclin-dependent kinase inhibitor at the G0–G1 transition of the cell cycle. In this case, as an ubiquitin ligase, RNF123 recognizes and mediates the ubiquitination of P27, while KPC2 interacts with ubiquitinated P27 to promote its degradation in the proteasome [34–36]. Recently, it has been reported that RNF123 mediated ubiquitination and degradation of NF-κB1 (p105) leading to repression of tumor growth [37]. Therefore, we set out to determine whether RNF123 functions as an important regulatory factor in antiviral innate immune responses and whether the E3 ligase activity of RNF123 is required for its regulatory action. Our results assign a function in RLR-mediated antiviral signaling to human RNF123 and highlight the emerging importance of a catalysis-independent role for RING finger family proteins.

Results

RNF123 overexpression inhibits RNA virus-induced responses

MDA5 is a RLR family member responding to certain kinds of RNA viruses like EMCV. It has not been sufficiently characterized how activation of MDA5 is regulated. We set out to identify MDA5 interactors by performing yeast two-hybrid screens with the MDA5 CARD as the bait. A RING finger protein RNF123, which has been reported to be an E3 ligase of P27, was identified in the human fetal kidney cDNA library. We first determined whether RNF123 influences RNA virus-induced responses. In luciferase reporter assays, overexpression of RNF123 apparently reduced SeV- and EMCV-induced activation of the IFN-β promoter in HEK293T cells. As a control, RNF123 had no effect on the overexpression of the cGAS- and STING-induced activation of the IFN-β promoter (Fig 1A). We also found that overexpression of RNF123 markedly decreased SeV-induced, but not the cGAS- and STING-induced, activation of the NF-κB promoter (Fig 1B).

In RT–PCR and qPCR experiments, overexpression of RNF123 inhibited SeV-induced, but not cGAS- and STING-induced, transcription of IFN-β and endogenous pro-inflammatory genes such as RANTES (Fig 1C and D). In bioassays, overexpression of RNF123 depressed the IFN-β secretion in HEK293T cells triggered by SeV infection, but not by overexpression of cGAS and STING (Fig 1E). These data suggested that RNF123 specifically inhibits IFN-β production induced by RNA but not DNA viruses.

In accordance with the above results, we found that overexpression of RNF123 enhanced NDV-eGFP (NDV-enhanced green fluorescent protein) replication in 293T cells (Fig 1F), while also enhancing the replication of EMCV in HeLa cells (Fig 1G). These data suggested that RNF123 inhibits RNA virus-triggered IFN-β production and cellular antiviral activity.

Knocking down of RNF123 prompts anti-RNA virus signaling

To confirm that endogenous RNF123 plays a role in anti-RNA virus signaling, we generated stable RNF123-knockdown cell pools using shRNA plasmids that targeted four sites on human RNF123 mRNA. Two shRNA plasmids (#3 and #4) markedly reduced the RNF123 mRNA level in HEK293T cells, while the #1 and #2 shRNA plasmids had no apparent effect (Fig 2A). In reporter assays, the knocking down of RNF123 (by #3 and #4) potentiated activation of the IFN-β and NF-κB promoters induced by SeV and EMCV but not by cGAS and STING, whereas #1 and #2 had no evident effect (Fig 2B and C). Knockdown of RNF123 accordingly leaded to improved transcription of endogenous IFN-β and RANTES induced by SeV or EMCV infection in RT–PCR

Figure 1. RNF123 overexpression inhibits RNA virus-induced responses.

A RNF123 suppresses the SeV- and EMCV-induced, but not the cGAS- and STING-induced, activation of the IFN-β promoter. HEK293T cells (3×10^5) were transfected with the expression plasmid for cGAS (50 ng) and STING (50 ng) or empty vector (100 ng), and 0, 50, 100, or 200 ng (wedges) of RNF123 (below lanes) together with the IFN-β reporter plasmid (100 ng) and the pRL-TK (100 ng) for 12 h, and then they were stimulated with SeV or EMCV or left untreated for 18 h. Luciferase assays were performed and results were presented compared to the luciferase activity in control cells.

B RNF123 inhibits SeV-induced, but not the cGAS- and STING-induced, activation of the NF-κB promoter. HEK293T cells were transfected with the indicated plasmids as in (A), together with the NF-κB reporter plasmid (100 ng) and the pRL-TK (100 ng) for 12 h, and the cells were then stimulated for 24 h with SeV or left untreated. Luciferase assay was performed as described in (A).

C, D RNF123 inhibits the SeV-induced, but not the cGAS- and STING-induced, RANTES and IFN-β transcription. HEK293T cells were transfected with cGAS (1 μg) and STING (1 μg) or empty vector for 12 h, then stimulated for 12 h with SeV, or left untreated. Total RNA was extracted and RT–PCR (C) or qPCR (D) was performed with the indicated primers.

E RNF123 inhibits the SeV-induced, rather than the cGAS- and STING-mediated, IFN-β secretion. The transfection and stimulation were done as in (A). Bioassays for type I interferon in the supernatants were performed and the results are presented compared to untreated control cells.

F Overexpression of RNF123 improves NDV-eGFP replication. HEK293T cells (1×10^5) were transfected with Flag-RNF123 plasmid or empty vector (2 μg). At 24 h after transfection, cells were infected with NDV-eGFP for 30 h, and fluorescence microscopy was used to visualize the GFP expression to determine the NDV replication. Cells were lysed and samples were detected using Western blot with GFP antibody. Scale bar: 100 μm.

G RNF123 enhances EMCV replication. HeLa cells (1×10^5) were transfected with Flag-RNF123 plasmid or empty vector (2 μg). At 24 h after transfection, cells were infected with EMCV or left untreated for 18 h. EMCV replication was determined using Western blot with VP1 antibody.

Data information: Each histogram shows the mean ± SD of three independent experiments done in triplicate. Asterisks indicate a significant difference level compared to the cells untransfected with RNF123 expression plasmids (Student's *t*-test, ***$P < 0.001$; **$P < 0.01$; *$P < 0.05$; ns, $P > 0.05$).

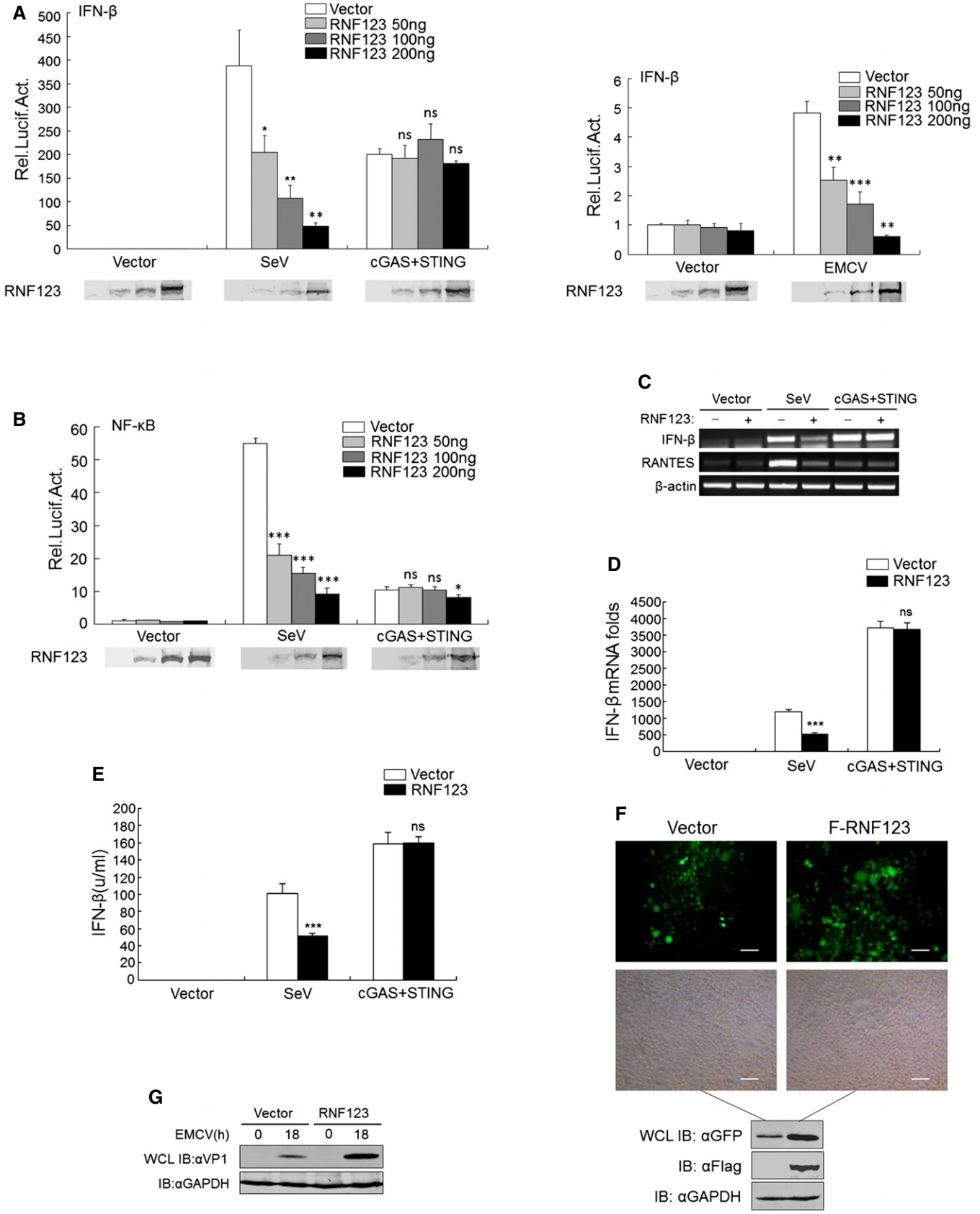

Figure 1.

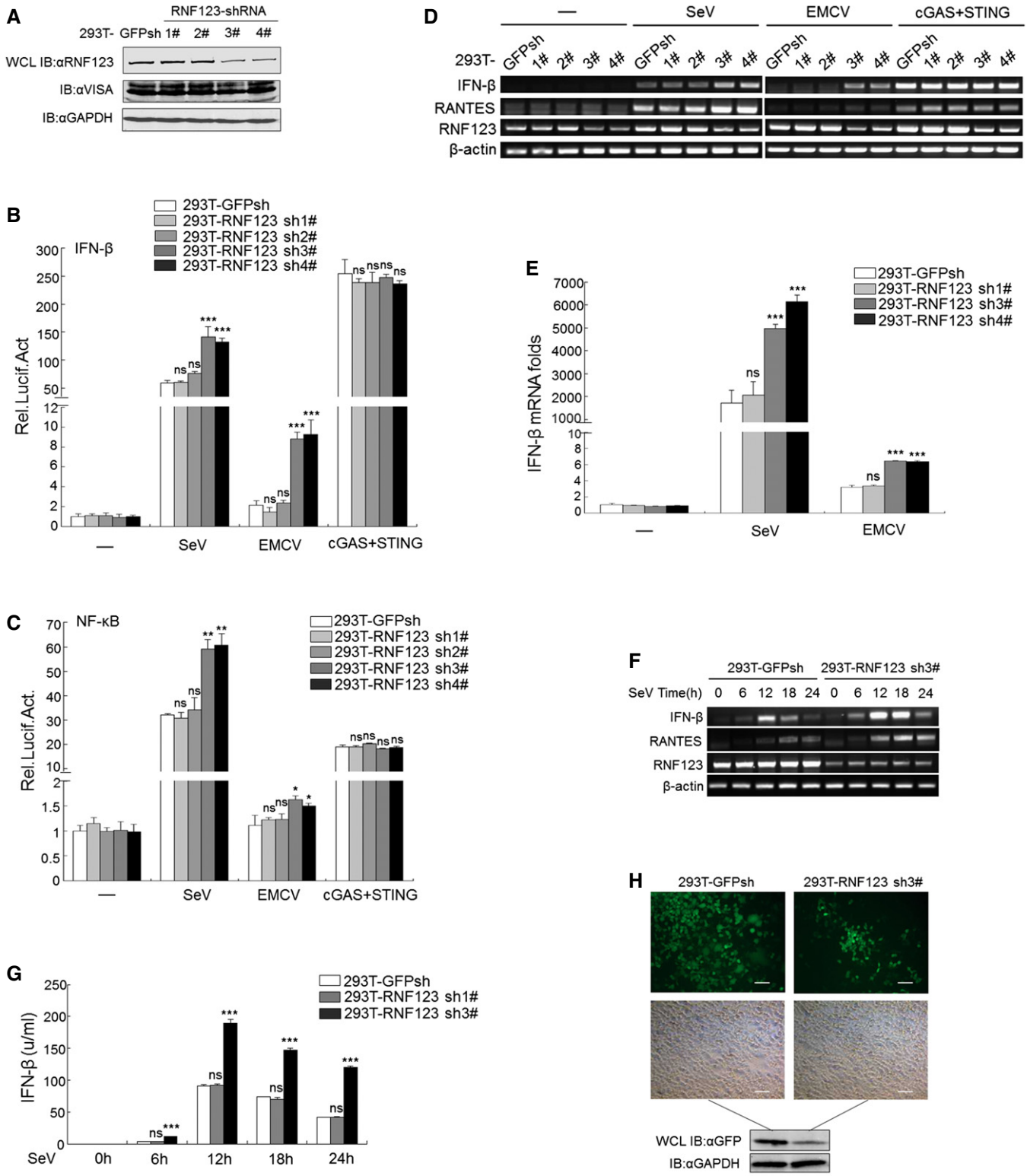

Figure 2.

experiments (Fig 2D), and qPCR experiments confirmed this quantitatively (Fig 2E).

We further determined the inhibitory role of endogenous RNF123 during the time course of viral infection. RT–PCR experiments showed that RNF123 knockdown improved the transcription of endogenous IFN-β and RANTES at 6 h after SeV infection, and this significantly increased at 12 and 18 h after SeV stimulation in HEK293T cells (Fig 2F). Also, in type I IFN bioassays, the

Figure 2. RNF123 knockdown potentiates anti-RNA virus signaling.

A Stable knockdown of RNF123 in HEK293T cells. HEK293T cells were infected with five lentiviruses encoding shRNA control (GFPsh) and four shRNAs targeting RNF123 (RNF123 sh #1, #2, #3, and #4). Western blot was performed with anti-RNF123, anti-VISA (as a control), and anti-GAPDH antibodies after selection.

B, C The RNF123 knockdown facilitated the activation of IFN-β and NF-κB promoters induced by SeV and EMCV but not by cGAS and STING. Stable HEK293T cells with GFPsh or RNF123 shRNAs (2×10^5) were transfected, infected with SeV or EMCV, and detected using luciferase assays as described in Fig 1A.

D, E Knockdown of RNF123 enhances the IFN-β and RANTES transcription induced by SeV and EMCV, but not that by the cGAS and STING. Stable HEK293T cells with GFPsh or RNF123 shRNAs were transfected and infected as in Fig 1C. Total RNA was extracted and RT–PCR (D) or qPCR (E) was performed with the indicated primers.

F, G Time course of potentiation of SeV-induced IFN-β transcription (F) and secretion (G) by the knockdown of RNF123. Stable HEK293T cells with GFPsh or RNF123 shRNAs were stimulated with SeV for 6, 12, 18, or 24 h, then total RNA was extracted, and RT–PCR was performed (F). Type I interferon bioassays were performed, and the results are presented compared to untreated control cells (G).

H Knockdown of RNF123 suppresses NDV-eGFP replication. Stable HEK293T cells with GFPsh or RNF123 shRNAs (2×10^5) were infected with NDV-eGFP. GFP expression was visualized and determined as in Fig 1F. Scale bar: 100 μm.

Data information: Each histogram shows the mean ± SD of three independent experiments done in triplicate. Asterisks indicate a significant difference level compared to 293T-GFPsh (Student's *t*-test, ***$P < 0.001$; **$P < 0.01$; *$P < 0.05$; ns, $P > 0.05$).

knockdown of RNF123 increased IFN-β secretion in HEK293T cells at 6, 12, 18, and 24 h after SeV infection (Fig 2G).

We also generated stable RNF123-knockdown pools of HeLa cells and obtained similar results. As shown by the Western blot analysis, RNF123 sh #3 and #4 inhibited RNF123 expression (Fig EV1A). The knockdown of RNF123 in HeLa cells also markedly improved the transcription of endogenous IFN-β at 12 h after SeV and EMCV infection in RT–PCR experiments (Fig EV1B). qPCR provided quantitative verification (Fig EV1C). These results suggested that RNF123 physiologically inhibits RNA virus-induced IFN-β production.

Next, we determined whether endogenous RNF123 is involved in cellular anti-RNA virus responses. Upon infecting with NDV-eGFP, the HEK293T cells knocking down RNF123 were resistant to NDV infection, and the amount of NDV-eGFP-positive cells was apparently decreased (Fig 2H). Knockdown of endogenous RNF123 in HeLa cells also reduced the replication of EMCV (Fig EV1D). The above results suggested that RNF123 negatively regulated cellular antiviral response induced by RNA viruses.

Knocking out of RNF123 potentiates IFN-β production induced by RNA viruses

To further determine the function of RNF123, we generated RNF123-knockout HEK293T cell line using the CRISPR/Cas9 system (Fig 3A). Consistent with knockdown results, depletion of RNF123 more significantly potentiated activation of the IFN-β promoter induced by SeV and EMCV, but not by cGAS and STING, whereas reconstitution of RNF123 could in turn dampened activation of IFN-β promoter (Fig 3B). RNF123 knockout also resulted in apparently improved transcription and secretion of endogenous IFN-β upon SeV and EMCV infection (Fig 3C and D). These results confirmed that RNF123 plays an inhibitory role in IFN-β induction by RNA viruses.

RNF123 targets RIG-I and MDA5 in the RLR signaling pathway

We further identified the molecular targets of RNF123 in the anti-RNA virus signaling pathway. In reporter assays, we found that overexpressed RNF123 dose dependently inhibited the activation of IFN-β and NF-κB promoters induced by full-length RIG-I, the CARD of RIG-I, and the CARD of MDA5 (Fig 4A and B). We also found that RNF123 partly reduced the VISA-induced activation of the IFN-β and NF-κB promoters, but did not inhibit TBK1 and constitutively activated IRF3-5D-induced activation of the IFN-β promoter, and also had no influence on activation of the NF-κB promoter induced by TAB2 or IKKβ (Fig 4A and B). Consistently, RNF123 knockdown in 293T cells potentiated the IFN-β promoter activation triggered by overexpression of RIG-I, RIG-I CARD, MDA5, and MDA5 CARD, but not by overexpression of VISA, TBK1, and cGAS/STING (Fig 4C), suggesting that RNF123 may target RIG-I and MDA5 in the RLR signaling pathway.

Then, we explore whether RNF123 associates with RIG-I and MDA5 using co-immunoprecipitation experiments. RNF123 plasmid with Flag tag and MDA5 plasmid with hemagglutinin (HA) tag were transfected into HEK293T cells. The co-immunoprecipitation results revealed that RNF123 specially associated with RIG-I and MDA5, but not with VISA, TBK1, or cGAS under the same conditions (Fig 4D).

We further determined whether RNF123 associates with RIG-I and MDA5 in physiological conditions and whether RNA virus infection has the effect on the interaction, by performing co-immunoprecipitation with the anti-RNF123 antibody in HEK293T and HeLa cells. The co-immunoprecipitation results showed that endogenous RIG-I interacted very weakly with endogenous RNF123 in unstimulated HEK293T cells. However, a distinct binding appeared at 9 h and was greatly enhanced at 18 h after SeV infection, and this phenomenon was partly due to the inducible expression of RIG-I (Fig 4E). In HeLa cells, we found that endogenous MDA5 had a weak interaction with RNF123, and this was enhanced upon EMCV stimulation (Fig 4F). These results suggested that RNF123 associates with RIG-I or MDA5 in a viral infection-inducible manner.

We next use immunofluorescence to identify the distribution of RNF123 in HeLa cells, and we found that the overexpressed and endogenous RNF123 was dispersively localized in the cytoplasm of HeLa cells, which was similar to the distribution pattern of RIG-I and MDA5 but not VISA (Fig 4G and H). Double immunofluorescence staining showed that the overexpressed and endogenous RNF123 overlapped with RIG-I and MDA5, while there was no co-localization between RNF123 and VISA (Fig 4G and H). We also detected their localizations with SeV or EMCV infection and obtained similar results (Fig EV2A and B). These data confirmed that RNF123 interacted with RIG-I and MDA5, rather than VISA in the RLR signaling pathway.

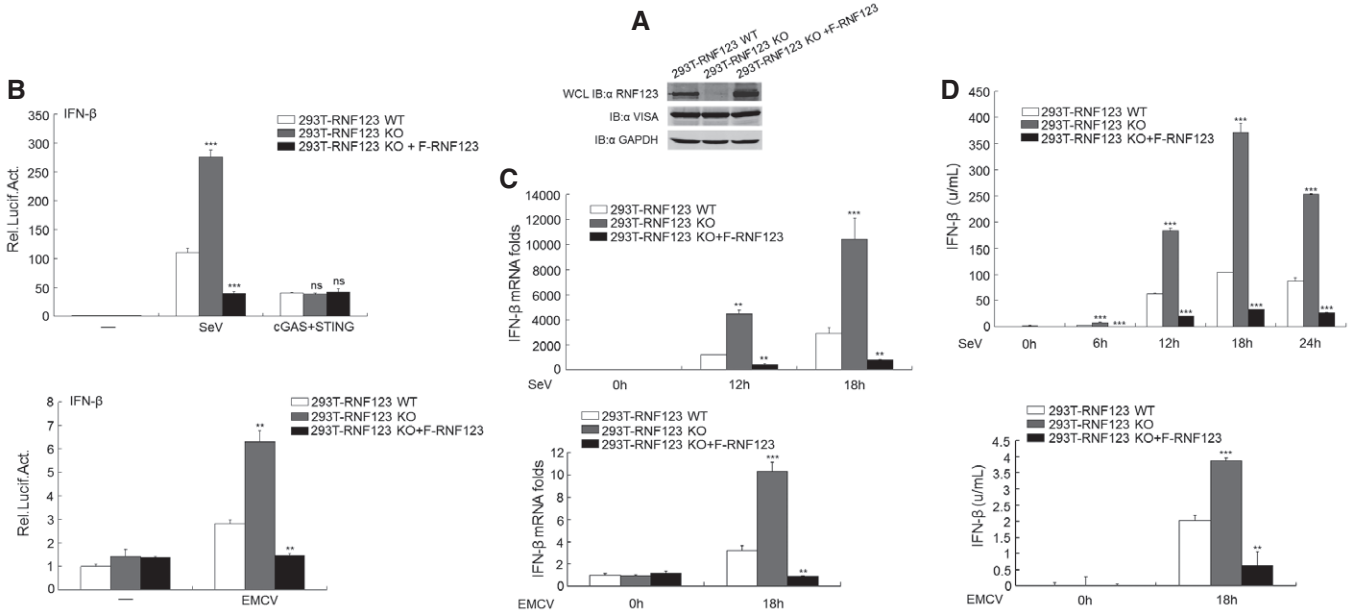

Figure 3. Knockout of RNF123 potentiates RNA virus-induced IFN-β production.

A RNF123 knockout and reconstitution in HEK293T cells. Knockout and reconstituted cells were detected using Western blot with anti-RNF123 and anti-VISA antibodies.

B Knockout of RNF123 facilitated the activation of IFN-β promoter induced by SeV and EMCV but not by cGAS and STING. The knockout and control cell lines (2×10^5) were transfected, stimulated with SeV or EMCV, and detected using luciferase assay as in Fig 1A.

C, D Knockout of RNF123 enhances the IFN-β transcription (C) and secretion (D) induced by SeV and EMCV. The knockout and control cell lines were stimulated with SeV or EMCV for the indicated time or left untreated. qPCR and type I interferon bioassays were performed as in Fig 1E and G.

Data information: Each histogram shows the mean ± SD of three independent experiments done in triplicate. Asterisks indicate a significant difference level compared to 293T-RNF123 WT (Student's *t*-test, ***$P < 0.001$; **$P < 0.01$; ns, $P > 0.05$).

The E3 ligase activity of RNF123 is not required for its inhibitory action

Since RNF123 has been reported to be an E3 ligase of p27 and NF-κB1 (p105) [34,37], we further clarified whether the E3 ligase activity is required for inhibiting RIG-I and MDA5. RNF123 contains an N-terminal SPRY domain, two coiled-coil domains in the middle, and a C-terminal RING finger domain [34] (Fig 5A). To determine which domain is crucial for its inhibitory function, we constructed RNF123 deletion mutants. In reporter assays, the truncation carrying the SPRY domain and two coiled-coil domains (residues 1–1,041) evidently suppressed activation of the IFN-β promoter induced by RIG-I CARD and MDA5 CARD as well as full-length RNF123, while the truncations carrying the SPRY, coiled-coil, or the RING domain alone had no inhibitory effect (Fig 5B). These results indicated that the SPRY and coiled-coil domains are both indispensable for the inhibitory action of RNF123, and the RING domain is not required. Co-immunoprecipitation analysis also showed that the truncation carrying the SPRY domain and two coiled-coil domains interacted with RIG-I CARD, while the other truncations did not (Fig 5C), confirming that the RING domain is not necessary for the interaction with RIG-I. Above results suggested that the RING domain of RNF123 is not required for the negative regulatory function in RLR signaling.

Previous studies have suggested that RNF123 requires a cofactor called KPC2 which together with RNF123 (also called KPC1) forms the active ubiquitin ligase complex KPC, promoting P27 degradation at the G1 phase of the cell cycle [34–36]. We therefore tested whether KPC2 is involved in the inhibitory function of RNF123. In reporter assays, overexpression of KPC2 alone in HEK293T cells had no evident effect on the activation of the IFN-β promoter induced by RIG-I CARD and MDA5 CARD, and co-transfection with RNF123 and KPC2 had the same inhibitory effect as RNF123 transfection alone (Fig 5D). To further determine the function of KPC2 in RLR signaling, we knocked down endogenous KPC2 expression in HEK293T cells using lentivirus-delivered shRNAs. As shown by the mRNA levels, two shRNAs (KPC2 shRNA #2 and #4) inhibited KPC2 expression comparing with shRNA control (GFPsh) (Fig 5E). We found that KPC2 depletion did not influence on SeV-induced activation of the IFN-β promoter, nor influence the inhibitory action of overexpressed RNF123 (Fig 5F). Knockdown of KPC2 also did not impact the transcription of endogenous IFN-β induced by SeV infection (Fig 5G). All the results indicated that KPC2 is not required for the inhibitory function of RNF123 in RLR signaling.

RNF123 inhibits RIG-I/MDA5 binding with VISA

RIG-I/MDA5 contains a conserved domain structure including a CARD domain at the N-terminus, a DExD-box RNA helicase domain, and a CTD. To further detect which domain of RIG-I/MDA5 is important for the interaction with RNF123, we co-transfected full-length (FL) or deletion mutants of RIG-I/MDA5 with RNF123 and

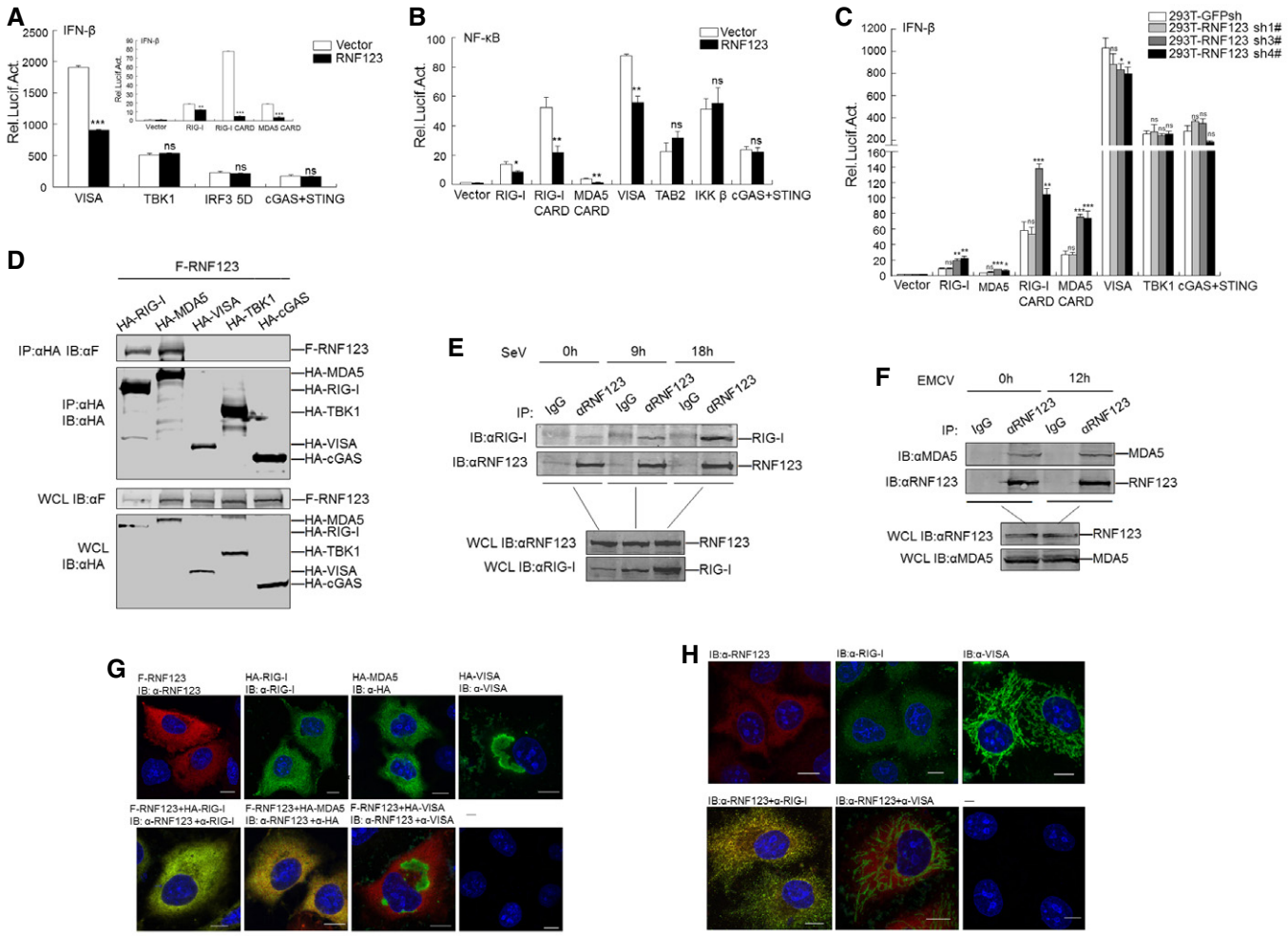

Figure 4. RNF123 targets RIG-I and MDA5 in the RLR signaling pathway.

A, B RNF123 inhibits the activation of the IFN-β (A) and NF-κB (B) promoters induced by the overexpressed RIG-I, RIG-I CARD, MDA5 CARD, and VISA, but does not affect the TBK1- and IRF3-5D-induced activation of the IFN-β promoter (A) and the TAB2- and IKKβ-induced activation of the NF-κB promoter (B). HEK293T cells (2×10^5) were transfected with the indicated reporter plasmids as in Fig 1A, together with an empty vector or Flag-RNF123 plasmid (100 ng). Luciferase assays were performed at 24 h after transfection.

C Knockdown of RNF123 potentiates the activation of the IFN-β promoter induced by overexpression of RIG-I, RIG-I CARD, MDA5, and MDA5 CARD, but not that by VISA, TBK1, and cGAS/STING. Stable HEK293T cells with GFPsh or RNF123 shRNAs (2×10^5) were transfected with the indicated plasmids. Luciferase assays were performed at 24 h after transfection.

D RNF123 associated with RIG-I and MDA5, but not with VISA, TBK1, and cGAS. Flag-RNF123 (F-RNF123) together with HA-RIG-I, HA-MDA5, HA-VISA, HA-TBK1, or HA-cGAS plasmids (8 μg each) was transfected into HEK293T cells (1×10^6). Cell lysates were immunoprecipitated (IP) with anti-HA (αHA). The immunoprecipitates and whole-cell lysates (WCL) were detected using Western blot (IB) with the anti-Flag (αF) or anti-HA antibody (αHA).

E Endogenous interaction between RNF123 and RIG-I upon SeV infection. HEK293T cells (3×10^6) were stimulated or left untreated for 9 or 18 h with SeV. Cell lysates were immunoprecipitated (IP) with IgG or with anti-RNF123 antibody. The immunoprecipitates and whole-cell lysates (WCL) were detected using Western blot with rabbit anti-RIG-I or anti-RNF123 antibody.

F Endogenous interaction between RNF123 and MDA5 upon EMCV infection. HeLa cells (3×10^6) were treated with EMCV for 12 h or left untreated. Cell lysates were immunoprecipitated with anti-RNF123 antibody or control IgG. The immunoprecipitates and whole-cell lysates (WCL) were detected using Western blot with anti-MDA5 or anti-RNF123 antibody.

G The distribution of overexpressed RNF123, RIG-I, MDA5, and VISA in HeLa cells. HeLa cells were transfected with the indicated plasmids (2 μg each). Immunofluorescence staining was performed with rabbit anti-RNF123 (red), goat anti-RIG-I (green), mouse anti-HA (green), and mouse anti-VISA (green) antibodies. Scale bar: 10 μm.

H The distribution of endogenous RNF123, RIG-I, and VISA. Untransfected HeLa cells stained with rabbit anti-RNF123 (red), goat anti-RIG-I (green), and mouse anti-VISA (green) antibodies. Scale bar: 10 μm.

Data information: Each histogram shows the mean ± SD of three independent experiments done in triplicate. Asterisks indicate a significant difference level compared to the cells untransfected with RNF123 construct (for A and B) or 293T-GFP sh (for C) (Student's *t*-test, ***$P < 0.001$; **$P < 0.01$; *$P < 0.05$; ns, $P > 0.05$).

performed co-immunoprecipitation assays. We found that RNF123 interacted with the RIG-I CARD or MDA5 CARD as well as RIG-I-FL or MDA5-FL, but it did not interact with the CARD deletion mutants of RIG-I/MDA5 (Fig 6A and B). We further found that the association between RNF123 and RIG-I CARD was enhanced by infection with SeV (Fig 6C). Above results suggested that RNF123 suppressed

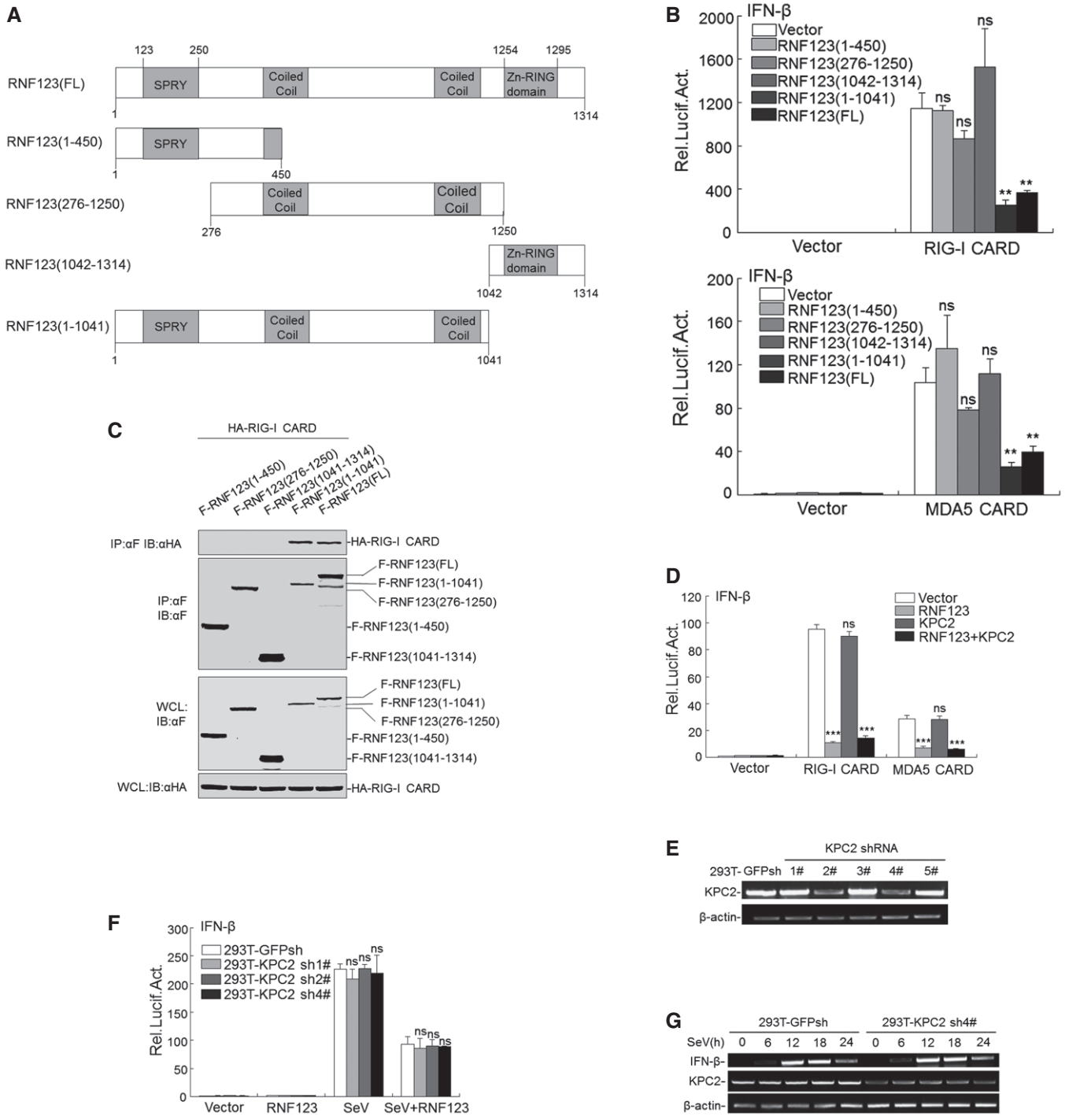

Figure 5.

RNA virus-induced responses by binding with the CARDs of RIG-I/MDA5.

It was known RIG-I/MDA5 CARD interacts with the VISA CARD to send signals downstream. We then predicted that RNF123 may impede the binding of RIG-I/MDA5 CARDs with VISA. In the co-immunoprecipitation assays, we found that the association of the RIG-I/MDA5 CARDs with VISA was markedly reduced when over-expression of RNF123 in HEK293T cells (Fig 6D and E). As a negative control, RNF123 did not influence the interaction between the RIG-I CARD and E3 ligase REUL, which is reported to associate with CARD of RIG-I (Fig 6F).

Then, we determined whether the endogenous interaction between RIG-I/MDA5 and VISA is enhanced when endogenous RNF123 is knocked down. We found that the endogenous interaction between RIG-I and VISA induced by SeV infection was intensely increased in RNF123-knockdown HEK293T cells (Fig 6G). Similar

Figure 5. The E3 ligase activity of RNF123 is not required for its inhibitory function in RLR signaling.

A The schematic structure of the full-length and the truncations of RNF123.

B The SPRY and coiled-coil domains, but not the RING domain, are indispensable for inhibiting IFN-β promoter activation. HEK293T cells (3×10^5) were transfected with the reporter plasmid as in Fig 1A and the indicated plasmids (100 ng). Luciferase assays were performed at 24 h after transfection.

C The SPRY domain and two coiled-coil domains of RNF123 are both required for interaction with RIG-I CARD. HEK293T cells (1×10^6) were transfected with HA-RIG-I CARD together with full-length or the truncations of RNF123 plasmids (8 μg each). Cell lysates were immunoprecipitated (IP) with anti-Flag (α-F). The immunoprecipitates were detected using Western blotting as described in Fig 4D.

D KPC2 has no effect on the activation of the IFN-β promoter induced by RIG-I CARD and MDA5 CARD. Transfection and luciferase assays were performed as described in Fig 4A.

E Effect of shKPC2 plasmids on endogenous KPC2. RT–PCR was performed with the indicated primers after HEK293T cells were infected with six lentiviruses encoding a shRNA control (GFPsh) and five shRNAs targeting KPC2 (Kpc2 #1-#5).

F KPC2 is not required for the inhibitory action of RNF123. Stable HEK293T cells (2×10^5) with GFPsh or KPC2 sh (#1, #2, or #4) were transfected and stimulated with SeV, and luciferase assays were performed as in Fig 1A.

G Knockdown of KPC2 had no effect on SeV-induced IFN-β transcription. Stable HEK293T cells with GFPsh or KPC2 sh #4 were stimulated with SeV for the indicated times, total RNA was extracted, and RT–PCR was performed.

Data information: Each histogram shows the mean ± SD of three independent experiments done in triplicate. Asterisks indicate a significant difference level compared to the cells transfected with vector (for B and D), or 293T-GFP sh (for F) (Student's *t*-test, ***$P < 0.001$; **$P < 0.01$; ns, $P > 0.05$).

results were obtained in EMCV-infected HeLa cells. The endogenous binding of MDA5 with VISA was also raised when RNF123 was knocked down (Fig 6H). Collectively, these data suggested that RNF123 inhibits the SeV- and EMCV-induced interaction between RIG-I/MDA5 and VISA.

Discussion

Type I IFNs have a broad-spectrum antiviral activity. However, the induction of IFNs must be accurately regulated; otherwise, it will result in inflammatory and autoimmune disease. A host of molecules has been shown as a positive or negative regulator of type I IFN induction by targeting RIG-I and MDA5, which are crucial cytosolic RNA sensors. For example, TRIM25 and REUL/Riplet, which are both E3 ubiquitin ligase of RIG-I, could catalyze lysine 63 (K63) ubiquitin ligation and specifically strengthen RIG-I-mediated signaling, while the E3 ligase RNF125 promotes RIG-I/MDA5 proteasomal degradation by conjugating K48 ubiquitin [26–30]. ARF-like protein 16 suppresses the association between RIG-I and RNA by means of binding with the CTD of RIG-I [38]. SEC14L1 could negatively regulate RIG-I through an inhibiting association of RIG-I with VISA [39]. RIG-I activity could also be regulated by phosphorylation or dephosphorylation. For example, protein kinase C α/β (PKC α/β) induces serine 8 phosphorylation at RIG-I CARD, and casein kinase (CK2) phosphorylates the CTD of RIG-I, which could strongly inhibit virus-induced production of IFN-β [40–42], whereas the primary phosphatases PP1α and PP1γ could activate MDA5/RIG-I via dephosphorylating them upon viral infection [43]. RAVERI specifically enhances the recognition of MDA5 and its upstream ligands [44]. And PIAS2β, which specifically SUMOylates MDA5, enhances the activation of MDA5 as well as the production of IFN-β [45].

With this research, we identified a RING finger family member RNF123 through a yeast two-hybrid screen. Overexpression of RNF123 inhibited SeV- and EMCV-triggered IFN-β production, while enhanced replication of RNA viruses. Knockdown or knockout of endogenous RNF123 facilitated SeV- and EMCV-induced IFN-β expression and inhibited EMCV and NDV replication in HEK293T and HeLa cells. The binding of RNF123 with the N-terminal CARDs of RIG-I/MDA5 depressed the interaction between RIG-I/MDA5 and VISA in both endogenous and exogenous situations. These results illustrated that RNF123 is a novel suppressor of RIG-I and MDA5.

In reporter assays, we also found that IFN-β and NF-κB promoters induced by VISA could be partly inhibited by overexpression of RNF123 (Fig 4A and B). Even so we do not consider VISA is the regulatory target of RNF123, because the knockdown of endogenous RNF123 specifically improved the activation of the IFN-β promoters induced by RIG-I/MDA5 instead of VISA. Co-immunoprecipitation experiments indicated that RIG-I and MDA5, but not VISA, associated with RNF123 (Fig 4D). It was also revealed through double immunofluorescence staining that overexpressed or endogenous RNF123 had a similar localization pattern with RIG-I and MDA5, while it had no overlap with VISA (Fig 4G and H). All these data confirmed that RIG-I/MDA5 are the major regulatory targets of RNF123 although we could not completely eliminate the possibility that RNF123 also has an impact on VISA.

Previous studies have shown that KPC (Kip1 ubiquitination-promoting complex), which consists of KPC1 (RNF123) and KPC2, ubiquitinates p27, and promotes its degradation [34,35]. In the capacity of an E3 ligase, RNF123 has also been reported to mediate the degradation of heterochromatin proteins 1α and β upon lamin A/C knockdown [46]. Recently, it was reported that the RNF123 could ubiquitinate NF-κB1 (p105) and mediate its proteasomal processing to p50 [37]. And another study showed that RKP, which is a homologue of RNF123 in plant cells, has an effect on plant virus infection through regulating the plant cell cycle [47]. These findings suggested that RNF123 participates in the regulation of the immune system. Our research indicated a novel innate immune function for RNF123, which plays a negative role in RIG-I-/MDA5-mediated signaling and the anti-RNA viral response.

We also revealed a different means by which RNF123 plays its role. Our data demonstrated that the RIG-I/MDA5 CARD-induced activation of the IFN-β promoter can still be suppressed through deletion of the RING domain (Fig 4B). On the contrary, the SPRY and two coiled-coil domains played vital roles in the association with RIG-I and the inhibition. These suggested the E3 ligase activity of RNF123 is not necessary for its inhibitory action. The other conclusion was that the inhibitory action of RNF123 on RIG-I/MDA5 does not rely on KPC2, which is an E3 ligase cofactor. We found that KPC2 depletion did not make a difference in SeV-induced activation of the IFN-β promoter; neither did it influence the inhibitory function of overexpressed RNF123 (Fig 4F). This is an instance of RNF123 performing an inhibitory function alone.

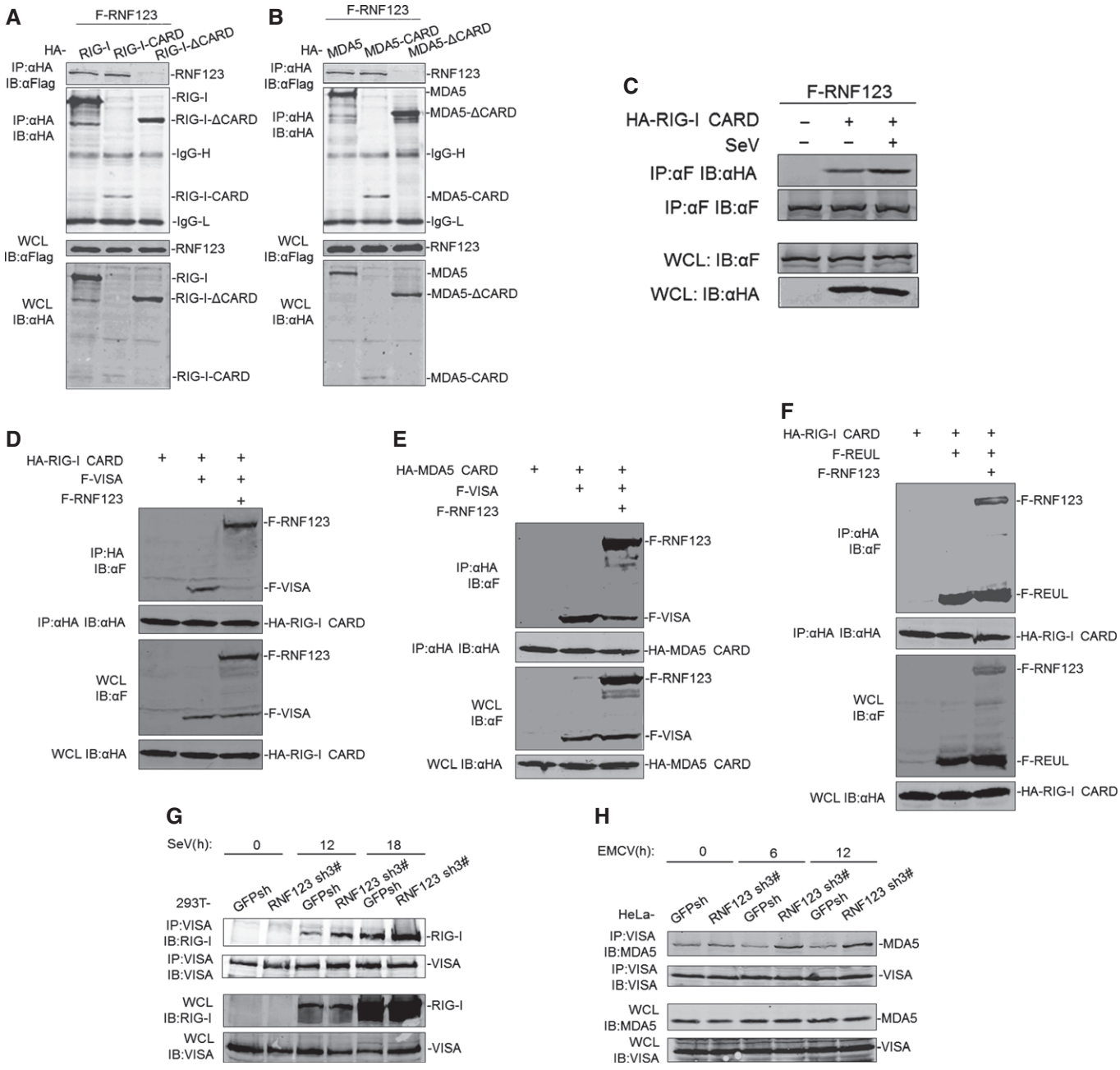

Figure 6. RNF123 inhibits RIG-I/MDA5 binding with VISA.

A, B RNF123 interacts with RIG-I CARD (A) and MDA5 CARD (B).

C SeV improves interaction between RNF123 and RIG-I CARD.

D, E RNF123 suppresses the binding of VISA with RIG-I CARD (D)/MDA5 CARD (E).

F RNF123 does not affect the interaction between RIG-I CARD and REUL.

G, H Knockdown of RNF123 facilitates the endogenous interaction between RIG-I (G)/MDA5 (H) and VISA. Stable HEK293T (G)/HeLa (H) cells with GFPsh or RNF123 shRNA were treated with SeV (G)/EMCV (H) for the indicated times. Cell lysates were immunoprecipitated with anti-VISA antibody. The immunoprecipitates and lysates were detected using Western blot with the indicated antibody.

Data information: In (A–F), HEK293T cells were transfected with the indicated plasmids. In (C), cells were stimulated with SeV or left untreated at 18 h after transfection. The co-immunoprecipitation and whole-cell lysates were detected as described in Fig 3D.

However, we are still not clear about the mechanism that triggers the interaction between RNF123 and RLR CARDs. We observed that the interaction between endogenous RNF123 and RIG-I/MDA5 was enhanced after SeV/EMCV infection (Fig 4E and F). And the association of overexpressed RNF123 with RIG-I CARDs also improved upon SeV infection (Fig 6C). As we did not found obvious changes

in the distribution pattern of RNF123 with SeV or EMCV infection (Figs 4G and H, and EV2A and B), we speculated that there were conformational changes or modifications of the RNF123 upon RNA virus infection, and these changes would improve the interaction between RNF123 and RIG-I/MDA5 CARDs. These speculations deserve further identify, especially using mass spectrography.

As RNF123 works with an inhibitory function in the RLR signaling pathway in human cells, we investigated whether it has an analogous effect in mouse cells. We knocked down endogenous RNF123 expression in L929 cells, employing mouse RNF123 shRNAs. To our surprise, we found that the mRNF123 knockdown did not affect the expression of endogenous IFN-β induced by SeV infection (Fig EV3A and B). We also generated a stable RNF123-knockdown pool of Raw264.7 cells and obtained similar results (Fig EV3C and D). These data suggested that RNF123 does not inhibit RIG-I/MDA5-induced anti-virus signaling in mouse cells. Therefore, we suspected that mRNF123 did not interact with mRIG-I. So we transfected HEK293T cells with the expression plasmids of HA-tagged mRNF123 and Flag-tagged mRIG-I and performed co-immunoprecipitation experiments. Unexpectedly, the results showed that mRNF123 still associated with mRIG-I, while as a negative control, mRNF123 had no interaction with mcGAS (Fig EV3E). So far, we have still not found the reasons for this phenomenon. We suspect that in mouse cells, there may exist a homologous molecule that plays a role redundant with RNF123. The answers to questions above may favor to the further identification of the functions of RNF123 and the regulatory mechanisms of the innate immune response.

Materials and Methods

Reagents and cell lines

Mouse antibodies against Flag (F3165) and HA (H9658) epitopes (Sigma-Aldrich, USA), IRDye800-conjugated anti-mouse (610-132-121) and anti-rabbit antibodies (611-131-002) (Rockland Immunochemicals, USA), mouse monoclonal anti-GAPDH (M20006) and anti-GFP antibodies (M20004) (Abmart, China), rabbit polyclonal antibodies against RNF123 (A7618), RIG-I (A0550) (Abclonal, China), and MDA5 (ab187303) (Abcam, USA), goat anti-RIG-I polyclonal antibody (sc-48929) (Santa Cruz, USA), mouse anti-VISA polyclonal antibody and SeV (Prof. Hong-Bing Shu, Wuhan University, China), mouse anti-VP1 polyclonal antibody and EMCV (Prof. Xin Guo, China Agriculture University, Beijing, China), NDV-eGFP (Prof. Cheng Wang, Institute of Biochemistry and Cell Biology, Shanghai, China), 2fTGH cell line (Prof. Zheng-Fan Jiang, Peking University, China), L929 cell line (Prof. Xiao-Feng Zheng, Peking University, China), HEK293T, HeLa, and Raw264.7 cell lines (Prof. Hong-Bing Shu, Wuhan University, China) were obtained from the indicated sources. Cell lines were grown in DMEM with 10% fetal bovine serum (Gibco, USA).

Constructs

Mammalian expression plasmids for Flag- or HA-tagged human RNF123, KPC2, RIG-I, MDA5, REUL, cGAS, and their deletion mutants, HA-tagged mouse RNF123, and Flag-tagged mouse RIG-I and cGAS were constructed using standard molecular biological techniques. Mammalian expression plasmids for Flag- or HA-tagged human VISA, TBK1, IRF3-5D (S396D, S398D, S402D, T404D, and S405D), STING, TAB2, IKKβ, IFN-β, and NF-κB promoter luciferase reporter plasmids were provided by Dr. Hong-Bing Shu (Wuhan University, Wuhan, China).

Yeast two-hybrid screens

Following the manufacturer recommended protocols, the human fetal kidney cDNA library (Clontech, USA) was screened using the MDA5 CARD as bait.

Transfection and luciferase assays

HEK293T cells were incubated on 24-well plates and transfected with 100 ng of firefly luciferase reporter plasmid with the expression plasmid or empty control vector together by standard calcium phosphate or polyetherimide precipitation. 100 ng of the Renilla luciferase reporter plasmid was transfected to each sample to normalize the transfection efficiency. Luciferase assays were measured using a dual-specific luciferase assay kit (Promega, USA). All reporter assays were repeated at least three times. The average value with standard deviation (SD) from three independent experiments is shown.

Co-immunoprecipitation and Western blot analysis

HEK293T cells (~2×10^5) were transfected with the indicated plasmids. At 20 h after transfection, cells were lysed in 1 ml of lysis buffer (20 mM Tris [pH 7.5], 1% Triton X-100, 150 mM NaCl, 1 mM EDTA, 1 mM phenylmethylsulfonyl fluoride, 10 mg/ml leupeptin, 10 mg/ml aprotinin). For each sample, 0.9 ml cell lysates were mixed with 1 μl indicated antibody and 25 μl protein A-Sepharose (GE Healthcare, USA) for 4 h at 4°C. The Sepharose beads were washed for three times with 1 ml of cold lysis buffer, and the proteins were eluted with 2× SDS sample buffer by boiling at 95°C for 10 min. Western blot was used to analyze the samples following standard protocol. The nitrocellulose membrane was incubated with indicated primary antibodies at 4°C for 12 h and then incubated with IRDye800-conjugated secondary antibodies (diluted 1:20,000), and the protein bands were visualized with an Odyssey infrared imaging system (LICOR Inc.).

RT–PCR and qPCR

Total mRNA was isolated from cells with TRIzol reagent (Tiangen Biotech) and reverse-transcribed into cDNA with a reverse transcriptase (Fermentas). PCR was performed to test the expression of endogenous IFN-β, RANTES, β-actin, RNF123, KPC2, and as control. cDNAs were also amplified by an ABI7300 Detection System (Applied Biosystems) using SYBR Green PCR Master Mix (Takara). The $2\text{-}\Delta\Delta C_t$ method was used to calculate relative expression levels normalized by β-actin in every self-contained sample. The gene-specific primers were as follows: hIFN-β: 5′-CCAA CAAGTGTCTCCTCCAA-3′ and 5′-ATAGTCTCATTCCAGCCAG-3′, hRANTES: 5′-CCTCGCTGTCATCCTCATTG-3′ and 5′-TACTCCCGAA CCCATTTCTT-3′, hRNF123: 5′-GTCTGCTTCTTACACCGGCT-3′ and 5′-GAGCTTGTCCTCTGTGTCCC-3′, hKPC2: 5′-CGAATGCAATGCTG

GACGAG-3′ and 5′-GAGTGGAACAACGCCACCTA-3′, hβ-actin: 5′-ACGTGGACATCCGCAAAGAC-3′ and 5′-CAAGAAAGGGTGTAACGCAACTA-3′, mRNF123: 5′-TCCGAGCAGAGATCTTCAGGAA-3′ and 5′-TGCAACCACCACTCATTCTGAG-3′, mIFN-β: 5′-TCCGAGCAGAGATCTTCAGGAA-3′ and 5′-TGCAACCACCACTCATTCTGAG-3′, mβ-actin: 5′-TGACGTTGACATCCGTAAAGACC-3′ and 5′-AAGGGTGTAAAACGCAGCTCA-3′.

Type I IFN bioassays

50 μl supernatants collected from the virus stimulated cells were added to the 2fTGH cells (stably transfected with type I IFN-sensitive luciferase vectors). After 4-h incubation, the 2fTGH cells were split and measured with luciferase assay.

Immunofluorescence staining

Cells attached to the slides were immobilized for 20 min with ice-cold methanol at −20°C and then washed three times with phosphate-buffered saline (PBS). The cells were incubated with 5% bovine serum albumin–PBS for 30 min in order to block the nonspecific binding, stained with an appropriate primary antibody in 1% bovine albumin–PBS for 2 h at 37°C, and then washed in PBS for three times and stained with Alexa Fluor 488-labeled goat anti-mouse IgG (A-11001), Alexa Fluor 594-labeled goat anti-rabbit IgG (A-11037), or Alexa Fluor 488-labeled donkey anti-goat IgG (A11055) (Thermo Fisher, USA) for 1 h at 37°C. For double staining, the Alexa Fluor 488-labeled donkey anti-goat IgG was firstly incubated alone. After that, the cells were stained for 15 min with 4′,6-diamidino-2-phenylindole (DAPI) and were observed using a confocal microscope (LSM 710 NLO and DuoScan System, Zeiss).

Generation of the stable knockdown cell pools

The plasmids which encode lentiviruses expressing short hairpin RNAs (shRNAs) (Sigma-Aldrich) were transfected into HEK293T cells with a three-plasmid system to produce lentivirus. The following shRNAs were used: hRNF123sh #1 (TRCN0000033894), hRNF123sh #2 (TRCN0000033895), hRNF123sh #3 (TRCN0000033896), hRNF123sh #4 (TRCN0000033897), hKPC2sh #1 (TRCN0000034264), hKPC2sh #2 (TRCN0000034265), hKPC2sh #3 (TRCN0000034266), hKPC2sh #4 (TRCN0000034267), hKPC2sh #5 (TRCN0000034268), mRNF123sh (TRCN0000190349) #1, mRNF123sh (TRCN0000217438) #2, and the control hairpin GFPsh. HEK293T, HeLa cells, L929 cells, or Raw264.7 cells which were seeded onto 6-well plates were cultured with 2 ml complete medium. After 18 h, 1 ml indicated lentivirus supernatant was added with 8 μg/ml polybrene. After 48-h incubation, the cells were treated with 10 mg/ml puromycin for 72 h, and then they were collected for Western blot analysis.

Generation of the RNF123-knockout cell line by CRISPR/Cas9

The lentiCRISPRv1 (Addgene Plasmid #49535) vector was engineered to express a guide RNA targeting RNF123 (5′-ACATTTGGACCAGTTGCTAC-3′) by standard techniques. For transfection, HEK293T cells were plated at 6×10^5 cells per well in a 6-well plate and transfected with lentiCRISPR-based plasmid. At 36 h post-transfection, cells were split with DMEM containing 0.5 μg/ml puromycin and selected for 7 days. Single clones were isolated. Gene knockout was assessed by Western blot analysis using the anti-RNF123 antibody.

Expanded View for this article is available online.

Acknowledgements
The authors thank the assistance of the Core Facilities at the School of Life Sciences, Peking University, for confocal microscopy. This work was supported by the National Natural Science Foundation of China (31170822 and 31470841).

Author contributions
SW designed and performed the experiments, and wrote the manuscript. Y-KY performed the initiating screen and participated in the generation of knockout cell line. TC, HZ, W-WY, and S-SS performed the experiments. Z-HZ provided funding and contributed with discussing the results. D-YC conceived the experiments, analyzed the data, and wrote the manuscript. All authors reviewed the manuscript.

Conflict of interest
The authors declare that they have no conflict of interest.

References

1. Kumar H, Kawai T, Akira S (2009) Pathogen recognition in the innate immune response. *Biochem J* 420: 1 – 16
2. Yoneyama M, Kikuchi M, Natsukawa T, Shinobu N, Imaizumi T, Miyagishi M, Taira K, Akira S, Fujita T (2004) The RNA helicase RIG-I has an essential function in double-stranded RNA-induced innate antiviral responses. *Nat Immunol* 5: 730 – 737
3. Kato H, Sato S, Yoneyama M, Yamamoto M, Uematsu S, Matsui K, Tsujimura T, Takeda K, Fujita T, Takeuchi O *et al* (2005) Cell type-specific involvement of RIG-I in antiviral response. *Immunity* 23: 19 – 28
4. Kato H, Takeuchi O, Sato S, Yoneyama M, Yamamoto M, Matsui K, Uematsu S, Jung A, Kawai T, Ishii KJ *et al* (2006) Differential roles of MDA5 and RIG-I helicases in the recognition of RNA viruses. *Nature* 441: 101 – 105
5. Pichlmair A, Schulz O, Tan CP, Naslund TI, Liljestrom P, Weber F, Reis e Sousa C (2006) RIG-I-mediated antiviral responses to single-stranded RNA bearing 5′-phosphates. *Science* 314: 997 – 1001
6. Hornung V, Ellegast J, Kim S, Brzozka K, Jung A, Kato H, Poeck H, Akira S, Conzeimann KK, Schlee M *et al* (2006) 5′-Triphosphate RNA is the ligand for RIG-I. *Science* 314: 994 – 997
7. Rothenfusser S, Goutagny N, DiPerna G, Gong M, Monks BG, Schoenemeyer A, Yamamoto M, Akira S, Fitzgerald KA (2005) The RNA helicase Lgp2 inhibits TLR-independent sensing of viral replication by retinoic acid-inducible gene-I. *J Immunol* 175: 5260 – 5268
8. Yoneyama M, Kikuchi M, Matsumoto K, Imaizumi T, Miyagishi M, Taira K, Foy E, Loo YM, Gale M Jr, Akira S *et al* (2005) Shared and unique functions of the DExD/H-box helicases RIG-I, MDA5, and LGP2 in antiviral innate immunity. *J Immunol* 175: 2851 – 2858
9. Lu C, Xu H, Ranjith-Kumar CT, Brooks MT, Hou TY, Hu F, Herr AB, Strong RK, Kao CC, Li P *et al* (2010) The structural basis of 5′ triphosphate

double-stranded RNA recognition by RIG-I C-terminal domain. *Structure* 18: 1032 – 1043

10. Kowalinski E, Lunardi T, McCarthy AA, Louber J, Brunel J, Grigorov B, Gerlier D, Cusack S (2011) Structural basis for the activation of innate immune pattern-recognition receptor RIG-I by viral RNA. *Cell* 147: 423 – 435
11. Cui S, Eisenächer K, Kirchhofer A, Brzózka K, Lammens A, Lammens K, Fujita T, Conzelmann KK, Krug A, Hopfner KP *et al* (2008) The C-terminal regulatory domain is the RNA 5′-triphosphate sensor of RIG-I. *Mol Cell* 29: 169 – 179
12. Kawai T, Takahashi K, Sato S, Coban C, Kumar H, Kato H, Ishii KJ, Takeuchi O, Akira S (2005) IPS-1, an adaptor triggering RIG-I- and Mda5-mediated type I interferon induction. *Nat Immunol* 6: 981 – 988
13. Meylan E, Curran J, Hofmann K, Moradpour D, Binder M, Bartenschlager R, Tschopp J (2005) Cardif is an adaptor protein in the RIG-I antiviral pathway and is targeted by hepatitis C virus. *Nature* 437: 1167 – 1172
14. Seth RB, Sun L, Ea CK, Chen ZJ (2005) Identification and characterization of MAVS, a mitochondrial antiviral signaling protein that activates NF-kappaB and IRF 3. *Cell* 122: 669 – 682
15. Xu LG, Wang YY, Han KJ, Li LY, Zhai Z, Shu HB (2005) VISA is an adapter protein required for virus-triggered IFN-beta signaling. *Mol Cell* 19: 727 – 740
16. Hou F, Sun L, Zheng H, Skaug B, Jiang QX, Chen ZJ (2011) MAVS forms functional prion-like aggregates to activate and propagate antiviral innate immune response. *Cell* 146: 448 – 461
17. Fitzgerald KA, McWhirter SM, Faia KL, Rowe DC, Latz E, Golenbock DT, Coyle AJ, Liao SM, Maniatis T (2003) IKKepsilon and TBK1 are essential components of the IRF3 signaling pathway. *Nat Immunol* 4: 491 – 496
18. Sharma S, tenOever BR, Grandvaux N, Zhou GP, Lin R, Hiscott J (2003) Triggering the interferon antiviral response through an IKK-related pathway. *Science* 300: 1148 – 1151
19. Li XD, Wu J, Gao D, Wang H, Sun L, Chen ZJ (2013) Pivotal roles of cGAS-cGAMP signaling in antiviral defense and immune adjuvant effects. *Science* 341: 1390 – 1394
20. Sun L, Wu J, Du F, Chen X, Chen ZJ (2013) Cyclic GMP-AMP synthase is a cytosolic DNA sensor that activates the type I interferon pathway. *Science* 339: 786 – 791
21. Wu J, Sun L, Chen X, Du F, Shi H, Chen C, Chen ZJ (2013) Cyclic GMP-AMP is an endogenous second messenger in innate immune signaling by cytosolic DNA. *Science* 339: 826 – 830
22. Gao P, Ascano M, Wu Y, Barchet W, Gaffney BL, Zillinger T, Serganov AA, Liu Y, Jones RA, Hartmann G *et al* (2013) Cyclic [G(2′,5′)pA(3′,5′)p] is the metazoan second messenger produced by DNA-activated cyclic GMP-AMP synthase. *Cell* 153: 1094 – 1107
23. Li X, Shu C, Yi G, Chaton CT, Shelton CL, Diao J, Zuo X, Kao CC, Herr AB, Li P *et al* (2013) Cyclic GMP-AMP synthase is activated by double-stranded DNA-induced oligomerization. *Immunity* 39: 1019 – 1031
24. Ishikawa H, Barber GN (2008) STING is an endoplasmic reticulum adaptor that facilitates innate immune signalling. *Nature* 455: 674 – 678
25. Zhong B, Yang Y, Li S, Wang YY, Li Y, Diao F, Lei C, He X, Zhang L, Tien P *et al* (2008) The adaptor protein MITA links virus-sensing receptors to IRF3 transcription factor activation. *Immunity* 29: 538 – 550
26. Gack MU, Shin YC, Joo CH, Urano T, Liang C, Sun L, Takeuchi O, Akira S, Chen Z, Inoue S *et al* (2007) TRIM25 RING-finger E3 ubiquitin ligase is essential for RIG-I-mediated antiviral activity. *Nature* 446: 916 – 920
27. Gao D, Yang YK, Wang RP, Zhou X, Diao FC, Li MD, Zhai ZH, Jiang ZF, Chen DY (2009) REUL is a novel E3 ubiquitin ligase and stimulator of retinoic-acid-inducible gene-I. *PLoS ONE* 4: e5760
28. Oshiumi H, Matsumoto M, Hatakeyama S, Seya T (2009) Riplet/RNF135, a RING finger protein, ubiquitinates RIG-I to promote interferon-beta induction during the early phase of viral infection. *J Biol Chem* 284: 807 – 817
29. Oshiumi H, Miyashita M, Inoue N, Okabe M, Matsumoto M, Seya T (2010) The ubiquitin ligase Riplet is essential for RIG-I-dependent innate immune responses to RNA virus infection. *Cell Host Microbe* 8: 496 – 509
30. Arimoto K, Takahashi H, Hishiki T, Konishi H, Fujita T, Shimotohno K (2007) Negative regulation of the RIG-I signaling by the ubiquitin ligase RNF125. *Proc Natl Acad Sci USA* 104: 7500 – 7505
31. Chen R, Zhang L, Zhong B, Tan B, Liu Y, Shu HB (2010) The ubiquitin-specific protease 17 is involved in virus-triggered type I IFN signaling. *Cell Res* 20: 802 – 811
32. Friedman CS, O'Donnell MA, Legarda-Addison D, Ng A, Cárdenas WB, Yount JS, Moran TM, Basler CF, Komuro A, Horvath CM *et al* (2008) The tumour suppressor CYLD is a negative regulator of RIG-I-mediated antiviral response. *EMBO Rep* 9: 930 – 936
33. Jounai N, Takeshita F, Kobiyama K, Sawano A, Miyawaki A, Xin KQ, Ishii KJ, Kawai T, Akira S, Suzuki K *et al* (2007) The Atg5 Atg12 conjugate associates with innate antiviral immune responses. *Proc Natl Acad Sci USA* 104: 14050 – 14055
34. Kamura T, Hara T, Matsumoto M, Ishida N, Okumura F, Hatakeyama S, Yoshida M, Nakayama K, Nakayama KI (2004) Cytoplasmic ubiquitin ligase KPC regulates proteolysis of p27(Kip1) at G1 phase. *Nat Cell Biol* 6: 1229 – 1235
35. Kotoshiba S, Kamura T, Hara T, Ishida N, Nakayama KI (2005) Molecular dissection of the interaction between p27 and Kip1 ubiquitylation-promoting complex, the ubiquitin ligase that regulates proteolysis of p27 in G1 phase. *J Biol Chem* 280: 17694 – 17700
36. Hara T, Kamura T, Kotoshiba S, Takahashi H, Fujiwara K, Onoyama I, Shirakawa M, Mizushima N, Nakayama KI (2005) Role of the UBL-UBA protein KPC2 in degradation of p27 at G1 phase of the cell cycle. *Mol Cell Biol* 25: 9292 – 9303
37. Kravtsova-Ivantsiv Y, Shomer I, Cohen-Kaplan V, Snijder B, Superti-Furga G, Gonen H, Sommer T, Ziv T, Admon A, Naroditsky I *et al* (2015) KPC1-mediated ubiquitination and proteasomal processing of NF-kappaB1 p105 to p50 restricts tumor growth. *Cell* 161: 333 – 347
38. Yang YK, Qu H, Gao D, Di W, Chen HW, Guo X, Zhai ZH, Chen DY (2011) ARF-like protein 16 (ARL16) inhibits RIG-I by binding with its C-terminal domain in a GTP-dependent manner. *J Biol Chem* 286: 10568 – 10580
39. Li MT, Di W, Xu H, Yang YK, Chen HW, Zhang FX, Zhai ZH, Chen DY (2013) Negative regulation of RIG-I-mediated innate antiviral signaling by SEC14L1. *J Virol* 87: 10037 – 10046
40. Maharaj NP, Wies E, Stoll A, Gack MU (2012) Conventional protein kinase C-alpha (PKC-alpha) and PKC-beta negatively regulate RIG-I antiviral signal transduction. *J Virol* 86: 1358 – 1371
41. Nistal-Villan E, Gack MU, Martínez-Delgado G, Maharaj NP, Inn KS, Yang H, Wang R, Aggarwal AK, Jung JU, García-Sastre A *et al* (2010) Negative role of RIG-I serine 8 phosphorylation in the regulation of interferon-beta production. *J Biol Chem* 285: 20252 – 20261

42. Sun Z, Ren H, Liu Y, Teeling JL, Gu J (2011) Phosphorylation of RIG-I by casein kinase II inhibits its antiviral response. *J Virol* 85: 1036 – 1047
43. Wies E, Wang MK, Maharaj NP, Chen K, Zhou S, Finberg RW, Gack MU (2013) Dephosphorylation of the RNA sensors RIG-I and MDA5 by the phosphatase PP1 is essential for innate immune signaling. *Immunity* 38: 437 – 449
44. Chen H, Li Y, Zhang J, Ran Y, Wei J, Yang Y, Shu HB (2013) RAVER1 is a coactivator of MDA5-mediated cellular antiviral response. *J Mol Cell Biol* 5: 111 – 119
45. Fu J, Xiong Y, Xu Y, Cheng G, Tang H (2011) MDA5 is SUMOylated by PIAS2beta in the upregulation of type I interferon signaling. *Mol Immunol* 48: 415 – 422
46. Chaturvedi P, Khanna R, Parnaik VK (2012) Ubiquitin ligase RNF123 mediates degradation of heterochromatin protein 1alpha and beta in lamin A/C knock-down cells. *PLoS ONE* 7: e47558
47. Lai J, Chen H, Teng K, Zhao Q, Zhang Z, Li Y, Liang L, Xia R, Wu Y, Guo H *et al* (2009) RKP, a RING finger E3 ligase induced by BSCTV C4 protein, affects geminivirus infection by regulation of the plant cell cycle. *Plant J* 57: 905 – 917

